Prediction of the weld shape in arc welding

A numerical modeling example in multiphysics coupling

Frédéric Roger* — Ky Dang Van**

** Unité de Mécanique, ENSTA*
Chemin de la Hunière
F-91120 Palaiseau
*** Laboratoire de Mécanique des Solides*
Ecole Polytechnique
F-91120 Palaiseau

ABSTRACT. *A numerical model of the arc welding process is presented. It deals with all arc welding process with and without filler metal (Gas Metal Arc Welding and Gas Tungsten Arc Welding). We consider the three dimensional modelling of the stationary weld pool with a free deformable surface. All coupled equations are solved by the finite volume method. We consider heat transfer ands fluid flow in the weld pool and the geometry of the free surface subjected to arc pressure and drop impact in GMAW. The location of the energy supplied by drops in the weld pool is assumed to be a function of the Weber number. Comparison with macrography shows a really good agreement of the model.*

RÉSUMÉ. *Un modèle numérique des procédés de soudage à l'arc est présenté. Il traite des procédés de soudage à l'arc avec et sans apport de matière (soudage MIG/MAG et TIG). Nous considérons la modélisation tridimensionnelle d'un bain de fusion stationnaire avec une surface libre déformable. Toutes les équations couplées sont résolues par la méthode des volumes finis. Nous considérons les transferts thermiques et l'écoulement dans le bain de fusion ainsi que la géométrie de la surface libre soumise à la pression d'arc et à l'impact des gouttes en soudage MIG/MAG. La position de l'énergie fournie par les gouttes dans le bain de fusion est supposée être une fonction du nombre de Weber. Des comparaisons avec des macrographies montrent un très bon accord du modèle.*

KEYWORDS: *arc welding, weld pool, drop impact, multiphysics, finite volume method.*

MOTS-CLÉS : *soudage à l'arc, bain de fusion, impact de gouttes, multiphysique, volumes finis.*

1. Introduction

The weld geometry in arc welding introduces stress concentration. Thus it plays an important role in fatigue strength of welded assembly [LIEU 00]. Most of the time fracture is located in weld toe which can be assimilated to a notch with a small tip radius. The aim of the numerical model of the weld pool behaviour during welding is to predict the thermal field which is coupled with the fluid flow in the weld pool [ZAC 89], and the thermo-metallurgical and mechanical behaviour of the structure. This coupling allows to predict the residual stress field but not the shape of the weld after solidification. The purpose of this study is to be able to predict the geometry of the free surface and the fusion zone of the weld for Gas Tungsten Arc Welding and Gas Metal arc welding. In the GMAW process, the filler metal is taken into account with mass conservation, impact pressure of drops on the free surface and energy contribution of drops in the weld pool.

A three dimensional model has been developped to simulate heat transfer and fluid flow in the weld pool under the electric arc. To reduce computing time we consider a stationary weld pool relatively to the welding electrode. This assumption is based on the regularity of the weld shape.

In our numerical model considers the weld surface is considered as deformable submitted to arc pressure and drop impact in GMAW. It is shown that the filler metal supply a significant ratio of the total welding energy. Watkins [WAT 89] propose an average ratio of 40% of the total welding power. This energy transfer is located at different depths in the weld pool. We consider an empirical formula relating the critical Weber number with the splashing depth of drops. Once this number is known, the location of the heat transfer is determined.

The model is divided in two parts. The first is devoted to the coupling between heat transfer ans fluid flow in the weld pool. The second part is devoted to the prediction of the free surface geometry of the weld pool. The fusion limit resulting from the first part is a boundary condition for the second part.

2. Modeling of the weld pool

Fluid flow of the molten metal has been recognised as an important part of the heat transfer during the welding process. However the mechanisms causing the fluid flow have not been clearly identified.

The driving forces for the convection in the weld pool are :

1. Electromagnetic force which are body forces resulting from interaction between the electric arc and the fluid flow ;

2. Buoyancy force driven by thermal gradient in the weld pool ;

3. Surface tension force induced by Marangoni effect driven by surface tension gradients resulting from thermal gradients ;

4. Arc drag force with arc plasma flow near the free surface.

In the model, all the three first effects are taken into account.

The calculation domain for solving the governing equations is shown in figure 1. The coordinate system (x,y,z) is linked to welding electrode and then move at the constant welding speed u_0 relatively to the workpiece. The coordinate system of the workpiece is (ξ, y', z).

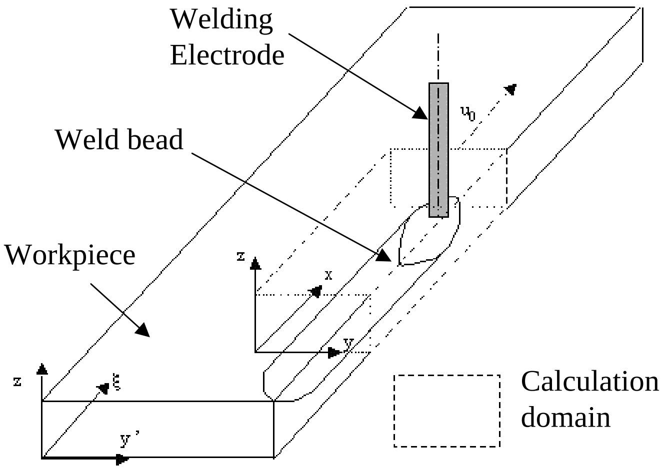

Figure 1. *Calculation domain moving with the welding electrode*

2.1. *Governing equations*

The governing equations for the temperature field and fluid flow are mass conservation, momentum conservation and energy conservation in the (x,y,z) coordinate system linked to the moving electrode. We consider a steady state of the fluid flow. The fluid is assumed viscous and incompressible. Laminar flow is assumed since the size of the pool is small. The thermophysical properties are assumed temperature dependant. Based on the above assumptions, the equations governing the weld pool can be expressed as follows :

Mass conservation :

$$\frac{\partial u}{\partial x} + \frac{\partial v}{\partial y} + \frac{\partial w}{\partial z} = 0 \qquad [1]$$

where u, v, w mean x, y and z-component of liquid metal velocity vector respectively.

Energy conservation :

$$\frac{\partial}{\partial x}(\rho C_p(u-u_0)T)+\frac{\partial}{\partial y}(\rho C_p vT)+\frac{\partial}{\partial z}(\rho C_p wT)=\frac{\partial}{\partial x}\left(k\frac{\partial T}{\partial x}\right)+\frac{\partial}{\partial y}\left(k\frac{\partial T}{\partial y}\right)+\frac{\partial}{\partial z}\left(k\frac{\partial T}{\partial z}\right)+S \qquad [2]$$

where S is a volumic heat source. In the model S corresponds to the heat supplied by drops in the GMAW weld pool.

Momentum conservation :

$$\rho\left((u-u_0)\frac{\partial u}{\partial x}+v\frac{\partial u}{\partial y}+w\frac{\partial u}{\partial z}\right)=-\frac{\partial p}{\partial x}+\mu\left(\frac{\partial^2 u}{\partial x^2}+\frac{\partial^2 u}{\partial y^2}+\frac{\partial^2 u}{\partial z^2}\right)+F_x \qquad [3]$$

$$\rho\left((u-u_0)\frac{\partial v}{\partial x}+v\frac{\partial v}{\partial y}+w\frac{\partial v}{\partial z}\right)=-\frac{\partial p}{\partial y}+\mu\left(\frac{\partial^2 v}{\partial x^2}+\frac{\partial^2 v}{\partial y^2}+\frac{\partial^2 v}{\partial z^2}\right)+F_y \qquad [4]$$

$$\rho\left((u-u_0)\frac{\partial w}{\partial x}+v\frac{\partial w}{\partial y}+w\frac{\partial w}{\partial z}\right)=-\frac{\partial p}{\partial z}+\mu\left(\frac{\partial^2 w}{\partial x^2}+\frac{\partial^2 w}{\partial y^2}+\frac{\partial^2 w}{\partial z^2}\right)+F_z-\rho g\beta(T-T_0) \qquad [5]$$

where, Fx, Fy and Fz mean x, y and z component of the electromagnetic force vector F, respectively. β is the thermal expansion coefficient.

We can noticed in these equations that the moving reference is take into account by the relative velocity term ($u-u_0$).

2.2. *Heat transfer*

Heat flux from arc is the major melting heat source. This heat is due to the electron flow and the convection from the plasma. In GMAW, the heat from overheated drops bring up to 40% of the total welding power.

The surface heat flux from the arc is assumed to have a gaussian distribution radially symmetrical around the electrode axis. Heat loss due to vaporization of the weld pool are take into account by a surface heat flux.

At the top of the weld pool, the thermal coupling with the plasma takes place in a thin layer wich is the anode boundary layer in GTAW and the cathode boundary layer in GMAW. This layer connects the arc plasma with the weld pool. We assume that this zone is a disc with a radius a. Ouside this zone we assume convection and radiation with the surrounding air.

Based on the above assumptions the heat flux at the top of the workpiece can be expressed as follows :

In the plasma contact zone :

$$-\lambda\frac{\partial T}{\partial z} = \eta q_0\, e^{-kr^2} - wH \qquad [6]$$

where λ is the thermal conductivity, r is the radial distance relatively to the electrode axis, η is the process efficiency, w is the vaporization rate ($g.m^{-2}.s^{-1}$) and H is the specific enthalpy of vaporization ($J.kg^{-1}$).

Around this zone :

$$-\lambda\frac{\partial T}{\partial z} = -\alpha\left(T - T_0\right) - \varepsilon\sigma\left(T^4 - T_0^4\right) \qquad [7]$$

In Gas Metal Arc welding, the melted electrode bring overheated drops. The depth of penetration in the weld pool depends on velocity before impact, drop diameter and surface tension. So we use the Weber number which is a ratio of kinetics energy of translation and surface free energy [ROG 00]. According to the value of the impact Weber number the impact is followed by a jet or a vortex in the weld pool. For high values (We>>1), kinetics energy is high and the drop impact is followed by a jet formation. For the low values (We<<1), the drop sinks and the energy is brought in depth. For mercury the critical number between the two modes is 8 [DAV 94].

We found a Weber number for steel electrode from 1,8 to 12,4 for welding current from 180 to 280 A [ROG00]. It is near the critical number for mercury. We decide to take surface heat source, like arc heat flux, for low Weber value and volumic heat source in the weld pool for high Weber value and then high welding current.

2.3. *Electromagnetic force field in the weld pool*

Electromagnetic force induced convection in the weld pool. The interaction between the electrical current flow and the magnetic induction creates a body force (Laplace force).

The magnetic induction field in the workpiece is created by the current flow in the workpiece and the arc plasma [ROG 01]. As the magnetic flux field through the weld pool surface is continuous, it is necessary to consider the combined effect of plasma and current in the workpiece to estimate the total magnetic field. Indeed, numerical results show that both effects are of the same order of magnitude [ROG 01]. The figure 2 shows the total Fx electromagnetic force component in the x direction along the weld pool. This figure shows the magnitude of the plasma induced force and the force induced by the current flow in the weld pool.

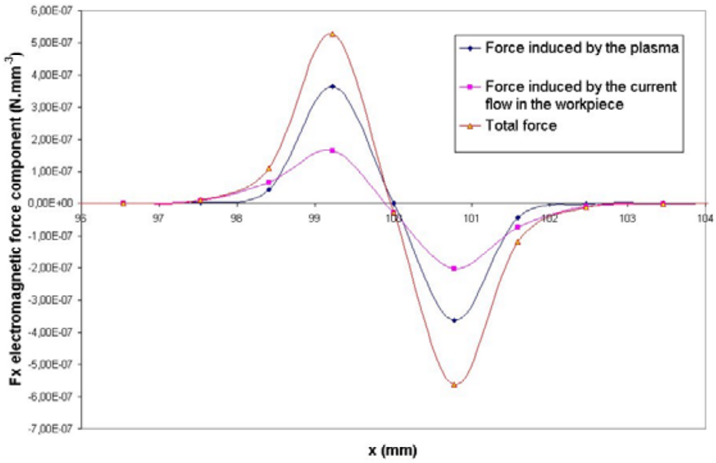

Figure 2. *Comparison between the force induced by the plasma and by the the current in the workpiece*

2.4. *Marangoni effect*

Streaming in a liquid due to a thermally caused surface tension gradient is called Marangoni effect. According to Ishizaki et al [ISHI66], circulation in a weld pool may partly be due to a surface tension gradient resulting from the temperature gradient in the molten metal. They support this view by model experiments with paraffin and stearic acid.

Small concentrations of surface active element affect weld pool shape by altering surface tension gradient on the weld pool surface [HEIP83] and thereby changing the magnitude and/or direction of fluid flow in the weld pool. According to the sign of the surface tension gradient, the fluid flow direction can change.

In the absence of significant concentration of surface active element, the surface tension of molten metals and alloys decreases with increasing temperature.

The figure 3 [ROG00] shows the fluid flow in a GTAW weld pool cross section for a negative and positive surface tension temperature coefficient.

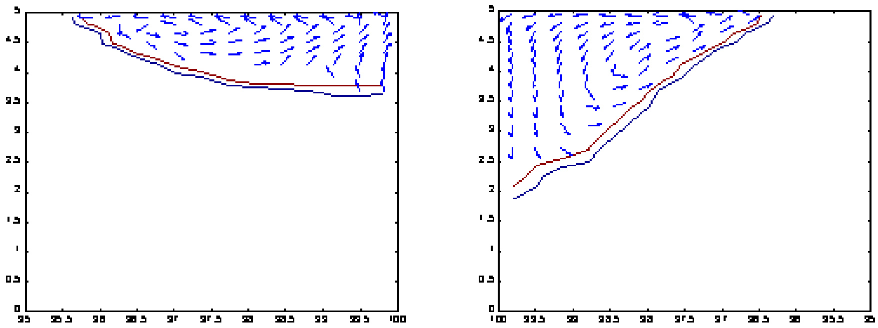

(a) (b)

Figure 3. *Fluid flow in the weld pool, (a) negative surface tension coefficient (-10^{-5} N/m.K) (b) positive surface tension temperature coefficient (10^{-5} N/m.K)*

Marangoni effect is take into account introducing Neumann boundary conditions on the velocity on the free surface [ZAC 89].

2.5. *Boundary conditions*

Boundary conditions for the temperature field and the fluid flow are summarized in figure 4. The calculation domain is symmetric along the (x,z) plane so we represent a half workpiece.

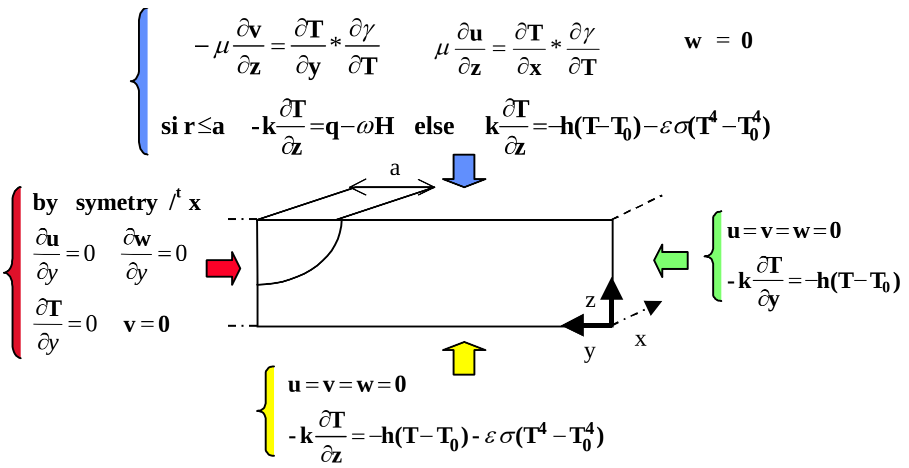

Figure 4. *Boundary conditions for velocity and temperature on a half workpiece*

3. Modeling of the deformable free surface

The weld free surface $\phi(x,y)=z(x,y)$ leans on the fusion line in front of weld pool and connects the solidified zone. We assume the solidified zone is regular so $\partial z/\partial x=0$. These limits define the geometric boundary condition for the calculation of the surface. Figure 5 shows these boundary conditions.

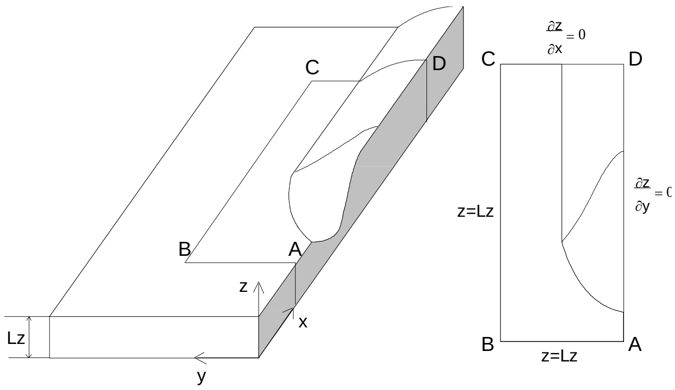

Figure 5. *Geometric Boundary conditions for the calculation of the free surface*

The geometric free surface equation can be deduced from the minimization of the free energy of the surface E_t subjected to the constraint of mass conservation with the filler metal. For GTAW, this energy is defined as follows :

$$E_t = \iint_S \left(\gamma \sqrt{1+\left(\frac{\partial \phi}{\partial x}\right)^2 + \left(\frac{\partial \phi}{\partial y}\right)^2} + \frac{1}{2}\rho g \phi^2 - Pa\phi \right) dxdy = \iint_S f\,.\,dxdy \qquad [8]$$

with E_t: total free energy (J), γ: surface tension ($N.m^{-1}$), Pa: arc pressure ($N.m^{-2}$).

Without filler metal the constraint equation is defined as follows :

$$\iint_S -\phi dxdy = \iint_S g.\,dxdy = 0 \qquad [9]$$

Using Euler-Lagrange's equation for the minimization of the free energy, we found the partial differential equation defined as follows :

$$P_a + \lambda - \rho g \phi = -\gamma \frac{\left(1+\phi_y^2\right)\phi_{xx} - 2\phi_x\phi_y\phi_{xy} + \left(1+\phi_x^2\right)\phi_{yy}}{\left(1+\phi_x^2+\phi_y^2\right)^{3/2}} \qquad [10]$$

With $\phi_x=\partial\phi/\partial x$, $\phi_{xy}=\partial^2\phi/\partial x\partial y$; λ is a Lagrangian multiplier that must be adjusted to respect the constraint [9].

In GMAW, we have a similar equation but we add the drop impact pressure P_g. Lagrange multiplier must be adjusted to take into account the amount of filler metal from the melted electrode. The governing equation for the surface is defined as follows :

$$P_a + P_g + \lambda - \rho g\phi = -\gamma\frac{\left(1+\phi_y^2\right)\phi_{xx} - 2\phi_x\phi_y\phi_{xy} + \left(1+\phi_x^2\right)\phi_{yy}}{\left(1+\phi_x^2+\phi_y^2\right)^{3/2}} \quad [11]$$

4. Numerical considerations

Figure 6 summarized coupling and boundary conditions. Calculation modules are framed with continuous lines. Interactions between the welding electrode wire, the electric arc and the weld pool are take into account with boundary conditions.

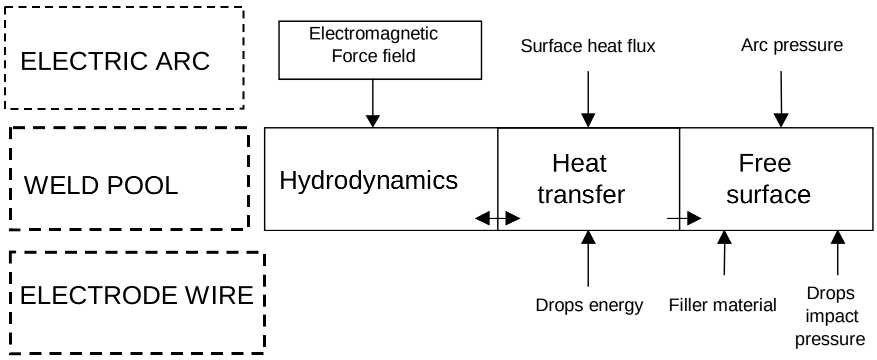

Figure 6. *Coupling and boundary conditions for the global model*

Governing equations for temperature field, fluid flow, electromagnetic force field and free surface geometry are solved by the finite volume method with a three-dimensionnal mesh. SIMPLER (Semi-Implicit Method for Pressure Linked Equations Revised) algorithm [PAT 80] is used to solve the coupling between continuity [1] and momentum equations [3,4,5]. An algorithm detects the weld pool zone location in the workpiece and solve the fluid flow only in this area. This algorithm reduces drastically the computing time to a few hours using a Personnal Computer.

5. Results and discussion

We present two applications of the model for GTAW and GMAW of medium thickness plates.

5.1. *Modeling of the Gas Tungsten Arc Welding*

Welding parameters are listed in table 1.

Steel plate Soldur 700 (C=0.068)	Plate thickness : 5 mm
Arc Voltage : 11,5 V	Current : 240 A
Welding speed : 3 mm/s	Electrode diameter : 2,4 mm
Arc length : 2 mm	

Table 1. *Welding parameters for GTAW*

Figure 7 shows a comparison between numerical simulation and a top view of the weld bead after solidification where the electric arc has been cut in stationary operating conditions. The simulation view shows stationary temperature field and fluid flow in the weld pool. The comparison is quite good as we found the top shape of weld pool.

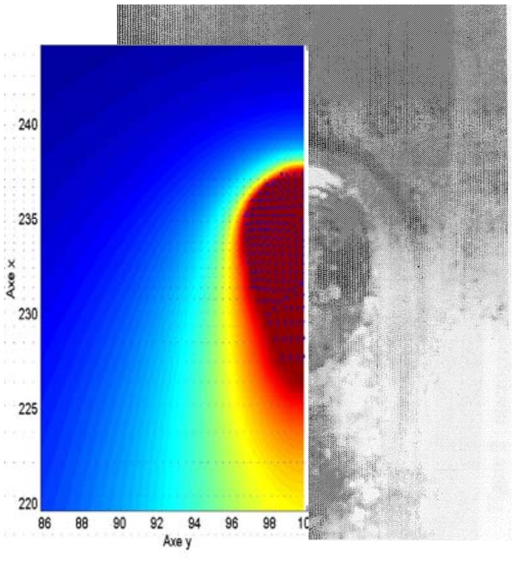

Figure 7. *Comparison between simulation and experiment for a top view of the plate in stationnary operating conditions*

5.2. *Modeling of the Gas Metal Arc Welding*

Welding parameters are listed in table 2.

Low carbon steel plate	Plate thickness : 6 mm
Arc voltage : 25 V	Current : 240 A
Welding speed : 430 mm/mn	Electrode diameter: 1,2 mm
Free electrode length : 16 mm	Gas composition : Ar – 2% CO_2

Table 2. *Welding parameters for GMAW*

We estimate the arc heat flux represent 45% of the welding power.This energy is distributed on a disc of radius 4mm.The drops energy is a assumed to be a volumic heat source distributed in a sphere with a diameter of 2mm (drops diameter predicted) at the depth of 3.5 mm. Figures 8 and 9 show numerical results and comparison with a macrography.

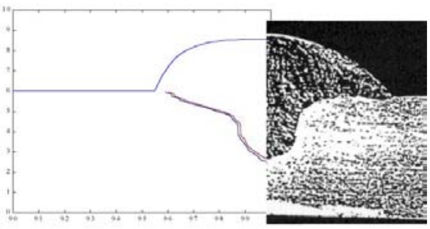

Figure 8. *Comparison between predicted shape and real shape in a macrography*

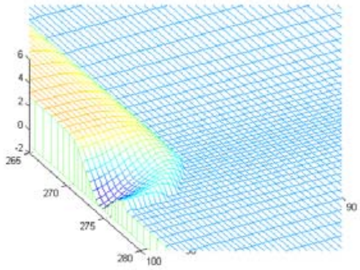

Figure 9. *View of the 3D stationary weld shape with pool depression*

It is necessary to developp a specific model for drop interaction to have a predictive weld shape. Figure 8 shows clearly that the drops influence weld pool penetration and dig a crater in the plate.

6. Conclusion

We have developped a global model to take into account multiphysics coupling in weld bead formation. Convective heat transfer in the weld pool plays a major role for the shape of the fusion zone for GTAW. In GMAW, filler metal plays also an important role because drops bring important energy, material and momentum.

We choose the finite volume method to discretize the governing equations. This method is well adapted for conservation equations with multiphysics coupling.

We reduce drastically computing time considering only the weld pool zone for the fluid flow calculations.

For the prediction of the free surface geometry, we solve a minimization problem under constraint. GTAW and GMAW models shows good agreement with experimental macrography of the weld shape.

The global model permits to study the influence of operating parameters on the weld pool shape and then to optimize it. The calculation of the free surface model permits to calculate the wetting angle of the weld which have a great influence on the fatigue behaviour of the welding assembly.

7. Bibliography

[DAV 94] Davis M. H., Painter M.J. Wahab M.A., "A source term for the computational modelling of the flow generated by a liquid droplet impiging on a liquid surface", *Computationnal Fluid Dynamics*, John Wiley & Sons, 1994.

[HEIP 83] Heiple C.R., Roper J.R., Stagner R.T., Aden J., "Surface active element effects on the shape of GTA, Laser, and Electron beam welds", *Welding Journal*, Welding research supplement, march 1983, p. 72s-77s.

[ISHI 66] Ishizaki K, Murai K., Kanbe Y, "Penetration in arc welding and -convection in molten metal", *International Institute of welding* (IIW), Doc 212-77-66.

[LIEU 00] Lieurade H. P., Huther I., « Introduction aux méthodes de dimensionnement à la fatigue des composants soudés », *Mécanique & Industries*, Volume 1, Issue 5, October 2000, p. 465-475.

[PAT 80] Patankar S. V., *Numerical Heat transfer and fluid flow*, Ed Hemisphere, New York, 1980.

[ROG 00] Roger F., Etude et modélisation de la formation d'un cordon de soudure à l'arc, Thèse de l'Ecole Polytechnique, Palaiseau, France, 2000.

[ROG 01] Roger F., Dang Van K., "Modelling the electromagnetic forces in a three dimensional GMAW weld pool", *Mathematical modelling of weld phenomena*, vol. 5, The institute of material, 2001.

[WAT 92] Watkins A.D., Smartt H.B., Johnson J.A., "A dynamic model of droplet growth and detachment in gmaw", *International trends in welding science and technology*, ASM, 1992, p. 993-997.

[ZAC 89] Zacharia T., Eraslan A.H., Aidun D.K., David S.A., "Three dimensional transient model for arc welding process", *Metallurgical Transaction B.*, Vol 20B, 1989, p. 645-659.